

Bandwidth broadening of X-ray free electron laser with the natural gradient of planar undulator

Minghao Song^{ab}, Jiawei Yan^{ab}, Kai Li^{ab}, Chao Feng^a and Haixiao Deng^{a*}

^a Shanghai Institute of Applied Physics, Chinese Academy of Sciences, Shanghai, 201800, People's Republic of China

^b University of Chinese Academy of Sciences, Beijing, 100049, People's Republic of China

Correspondence email: denghaixiao@sinap.ac.cn

Funding information National Natural Science Foundation of China (award Nos. 11475250, 11322550); China Association for Science and Technology; Ten Thousand Talents Program

Abstract Besides the target to pursue the narrow bandwidth X-ray pulses, the large bandwidth free-electron laser pulses are also strongly demanded to satisfy a wide range of scientific user experiments. In this paper, using the transversely tilt beam enabled by deflecting cavity and/or corrugated structure, the potential of large bandwidth X-ray free-electron lasers generation with the natural gradient of the planar undulator are discussed. Theoretical predictions and numerical simulations demonstrated that X-ray bandwidth exceeding 5% can be observed with the optimized free-electron laser parameters.

Keywords: Large bandwidth; deflecting cavity; corrugated structure; natural gradient

1. Introduction

X-ray free-electron laser (FEL) facility as the primary candidate for fourth-generation light source that holds the promise to provide extremely bright X-ray photons with femtosecond pulse duration. The leading-edge instruments offer several capabilities in a wide range of

scientific applications in chemistry, biology, material science and physics (Barletta *et al.*, 2010; Öström *et al.*, 2015). Currently, the operated or constructed FEL facilities around the world are generally based on the self-amplified spontaneous emission (SASE) (Emma *et al.*, 2010; Ishikawa *et al.*, 2012; Ackermann *et al.*, 2007; Kondratenko & Saldin, 1980; Bonifacio *et al.*, 1984) and seeded (Deng & Feng, 2013; Yu, 1991; Stupakov, 2009) FEL schemes. SASE FELs produce coherent radiation with final natural bandwidth between 10^{-3} and 10^{-4} (Bonifacio *et al.*, 1984), while the seeded FELs even further reduce the natural bandwidth to the Fourier transform limit (Zhao *et al.*, 2012; Amann *et al.*, 2012; Saldin *et al.*, 2001).

However, besides aiming at minimizing the bandwidth of the produced radiation, large bandwidth FEL pulse is also of great interest. With the help of the ultra-brightness of X-ray FEL and generation of broad bandwidth, it shows promise for revealing essence of molecular structures and solving remained problems, which will facilitate the progress in a variety of research fields, for example, studying microcrystalline materials (Catherine *et al.*, 2015; Baradaran *et al.*, 2013), analysing single-cell (Patterson *et al.*, 2010), determining multi-wavelength anomalous diffraction (MAD) phase information (Son *et al.*, 2011). Moreover, compared with standard narrow bandwidth operation, large bandwidth FEL allows for wavelength tuning in a more flexible way. More recently, large bandwidth FEL schemes were newly proposed (Prat *et al.*, 2016; Hernandez *et al.*, 2016), which mainly relies on the electron beam energy chirp formed in linear accelerators and/or the transverse gradient undulator.

The generation of FEL relies on the relativistic electron beam moves along a periodic array of dipole magnets and wiggled transversely to emit electromagnetic radiation (Madey, J. M. J., 1971; Kondratenko & Saldin, 1980; Huang & Kim, 2007). According to FEL resonant condition, both time-energy correlation in the electron bunch and space-field correlations in the undulator can broaden the FEL bandwidth. Generally, the simplest and natural way to obtain large bandwidth FEL is using an energy chirped electron beam (Andonian *et al.*, 2005). However, large energy chirp will be hindered and challenged for the X-ray FEL. Apart from it, there are many other approaches to produce the energy chirp, for instance, utilizing the space charge effects of an extremely compressed beam (Serkez *et al.*, 2013), modifying the

longitudinal laser profile of photo injector (Penco *et al.*, 2014) and using the over-compressed beam combined with wakefields (Hernandez *et al.*, 2016; Emma, 2000; Turner *et al.*, 2015). Alternatively, the application of transverse gradient undulator may contribute a full bandwidth of 10% in soft X-ray of 1 nm wavelength (Prat *et al.*, 2016; Bernhard *et al.*, 2016). Motivated by these early works, in this paper, X-ray FEL bandwidth broadening enabled by the natural gradient (vertical gradient usually) in a planar undulator is studied utilizing currently existed instruments and mature accelerator technologies. It is demonstrated that a full bandwidth from 2% to 5% could be obtained in hard X-ray region of 0.1 nm. Moreover, if the required X-ray pulse energy is not very high in some user experiments, i.e., FEL saturation is not mandatory, full bandwidth over 10% can be achieved in simulation.

2. Principle of scheme

In this paper, in condition to the techniques mentioned above, a simple scheme which consists of transverse-longitudinal coupling section and planar undulator section is proposed. As illustrated in Fig. 1, a de-chirper device (Fu *et al.*, 2015; Deng *et al.*, 2014; Bane *et al.*, 2016; Zagorodnov *et al.*, 2015; Zhang *et al.*, 2015; Emma *et al.*, 2014; Novokhatski, 2015) or transverse deflecting structure (TDS) (Akre *et al.*, 2001; Tan *et al.*, 2014) is installed before the undulator to introduce a vertical tilt to the electron beam. It is expected that such a beam passes through a planar undulator and produce FEL radiation with large bandwidth. The initial electron beam has the following properties depending on the FEL lasing requirements, 6 GeV beam energy and 3 kA peak current can be delivered with 200 pC bunch charge, with sliced emittance less than 0.3 μm -rad to satisfy the desired photon output. In this scheme, it is convenient to change the gap of de-chirper or deflecting voltage of TDS, thus the beam will experience different transverse kick and can be characterized with various tilt amplitudes, then one can simply tune the FEL bandwidth. In principle, the longitudinal wakefield of the corrugated structure could be used to further increase the beam energy chirp, and thus the FEL bandwidth.

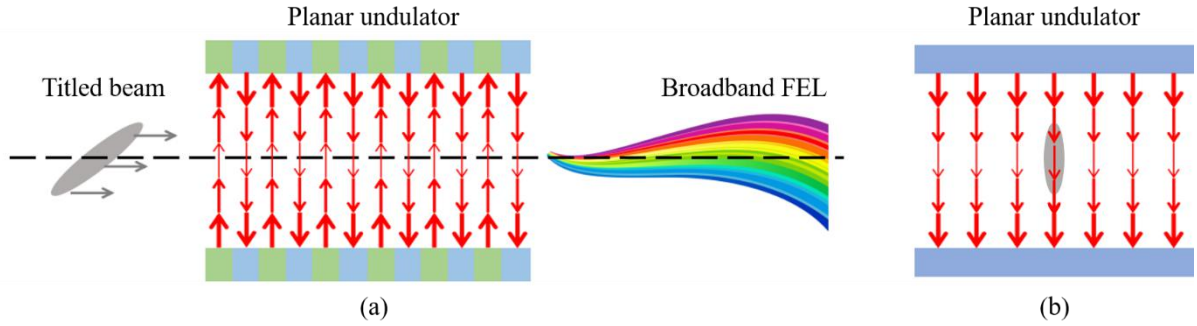


Figure 1

The schematic layout of the proposed scheme: (a) the titled beam travelling through the planar undulator with natural gradient to produce broad bandwidth FEL pulse and (b) displays the vertical magnetic field of undulator cross section.

2.1. Generation of beam transverse tilt

As aforementioned, an electron beam with a transverse tilt travelling through a planar undulator produces broad bandwidth X-ray FEL pulse. The beam transverse tilt can be generated with several methods. For example, applying a RF deflector to kick beam or introducing the transverse wakefields of accelerating structures or corrugated structures in the FEL facility.

The RF deflecting cavities have been widely used in the beam diagnostics of FEL and many other accelerators (Korepanov *et al.*, 2006; Park *et al.*, 2015; Akre *et al.*, 2001; Xiang *et al.*, 2010; Ding *et al.*, 2014; Lee *et al.*, 2014). In the deflecting cavity, the deflecting voltage is zero for the longitudinal centre of the bunch and provides a linear transverse deflection to the rest of the bunch, according to the (Alesini *et al.*, 2006), the transverse displacement of the bunch slice is proportion to the deflecting voltage, thus, the beam transverse tilt can be easily tuned through the deflecting voltage of the TDS structures. For example, a total power of 40 MW will be fed to a pair of X-band deflecting structures (Tan *et al.*, 2014) for SXFEL. Therefore, a wide range of transverse tilt could be achieved. Here a typical Gaussian electron bunch is used to explain. Fig. 2 represents the t - y phase space of the electron beam with 0.5 mm vertical tilt amplitude. It can be achieved by a 40 MV deflecting voltage together with a 14 meters drift, which has been verified by the ELEGANT (Borland, 2000) simulation.

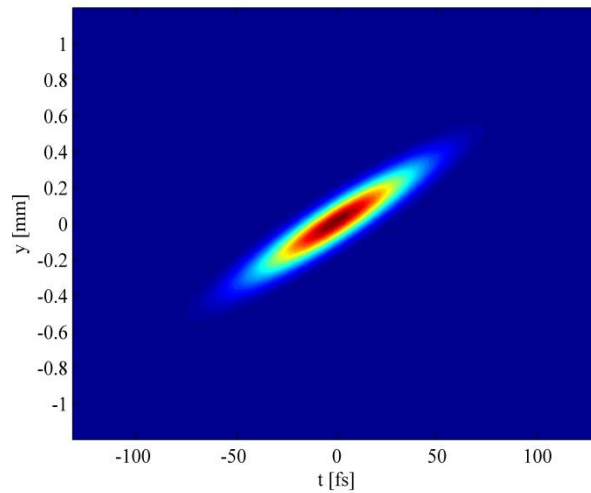


Figure 2

The simulated electron beam after the deflecting and drifting, the plot is the bunch phase space with vertical tilt amplitude of 0.5 mm. The bunch head is in the left.

A corrugated structure is usually a pipe or a pair of parallel plates with small bumps on the wall in a form of periodic ridges (Fu *et al.*, 2015; Deng *et al.*, 2014; Bane *et al.*, 2016; Zagorodnov *et al.*, 2015; Zhang *et al.*, 2015; Emma *et al.*, 2014; Novokhatski, 2015). When interacting with the longitudinal wakefields, the corrugated structures mainly responsible for beam energy chirp. While if the electron beam enters the structure with an offset from the axis, travelling close to one jaw of the structure, it excite the transverse dipole wakefields, where the bunch head receive no kick while the bunch tail will be transversely kicked. On the basis of the wakefield theory (Bane *et al.*, 2016; Zhang *et al.*, 2015; Novokhatski, 2015), it is interesting note that the bunch tail would experience a larger transverse kick with farther distance away from axis, in condition, the transverse tilt amplitude could be also simply tuned by varying the gap of the structure. Recently, on the basis of transverse beam tilt generated by the de-chirper at LCLS, a set of multi-colour X-ray FEL experiments was successfully accomplished (Lutman *et al.*, 2016). For the large bandwidth FEL application the corrugated structure has small gap of millimetre order. In the broad bandwidth X-ray FEL case here, if a beam vertical tilt of ± 0.5 mm is required, roughly it can be achieved when the electron beam passes through a 2.5 meter long LCLS similar corrugated structure with a vertical offset of 0.64 mm.

2.2. Natural gradient of a planar undulator

Considering a planar undulator in which the magnetic field in the vertical direction:

$$B(y) = B_0 \left(1 + \frac{1}{2} k^2 y^2\right) \quad (1)$$

Here $k=2\pi/\lambda_u$, λ_u is the undulator period and B_0 is the peak magnetic field. When a relativistic electron entering into the undulator, it will wiggle periodically in the horizontal x direction and emit radiation with the resonant wavelength (Huang & Kim, 2007). If one neglects the high order term $k^4 y^4$, one can derive that:

$$\lambda(y) = \lambda_0 + \frac{\lambda_u}{2\gamma_0^2} \cdot \frac{K_0^2}{2} \cdot k^2 y^2 \quad (2)$$

Here K_0 is the dimensionless undulator parameter and γ_0 is the electron energy in units of the electron rest energy. The FEL wavelength deviation in terms of the resonant wavelength λ_0 can be concluded:

$$\frac{\lambda(y) - \lambda_0}{\lambda_0} = \frac{K_0^2}{2 + K_0^2} k^2 y^2 \quad (3)$$

2.3. Weak focusing lattice

The electron beam size in the undulator has a great influence on FEL lasing. On the one hand, large beta function will enlarge the electron beam transverse cross section, which leads to the reduction of the current density and FEL gain, on the other hand, small beam size will cause radiation diffraction and increase the gain length (Xie, 1995; Jia *et al.*, 2004). Therefore, optimization of the beam Twiss function is important for the FEL performance. In general, the undulator section will be interrupted by several pairs of focusing quadrupoles and de-focusing quadrupoles to control the beam transverse size, which is well-known FODO lattice (Wiedemann, 2008). According to the Eq. (3), it is not difficult to find that the FEL bandwidth in the proposed scheme is proportional to the square of y , which means the vertical distance away from the axis. Obviously, the strong vertical oscillation of beam motion has an impact on the exponential gain and coherence building, and further affects the generated FEL bandwidth. Therefore, a weak focusing FODO lattice is preferred here.

Fortunately, the intrinsic vertical focusing effect of the planar undulator is quiet weak. If all the quadrupoles in the undulator system are set to be weakly focusing in horizontal, a periodic and controllable beta oscillation can be ensured and achieved in both horizontal and vertical direction. As shown in Fig. 3, an equivalent FODO lattice with length of 10 m consisting of focusing quadrupole, drift and a pair of planar undulator is considered, of which the undulator is 4.5 m long with period of 15 mm and K_0 of 1.47. Based on the transfer matrix of FODO cell, the properties of the beta function can be derived. Under such FODO cell, it is deserved to note that β_y variation is well controlled according to Fig. 3. More specifically, the difference between the maximum and minimum β_y is less than 2 m, which is truly small when compared with the averaged β_y about 230.

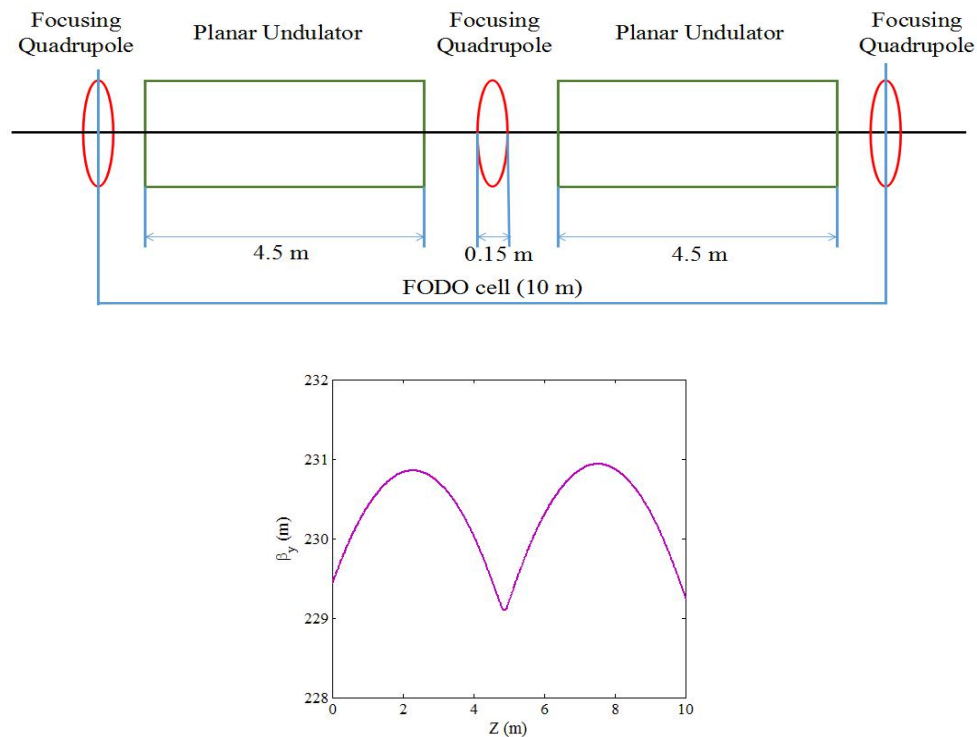


Figure 3

The equivalent FODO cell and corresponding vertical beta oscillation along the longitudinal direction.

2.4. Beam tilt control in undulator

For the proposed scheme, according to the aforementioned, the beam vertical oscillation is indeed not so strong because of a weak focused lattice. However, due to the residual vertical

focusing strength, vertical kick given by the TDS system and/or transverse wakefields, the vertical size of electron beam will slowly varies in the planar undulator, hence the generated FEL bandwidth would be narrowed and deviated from the expected. Fortunately, one can minimize the beam tilt variation by controlling the parameters of the whole system.

The undulator system can be roughly treated as an equivalent quadrupole with the focusing strength k_f which is determined by the detailed FODO structure, and the total length of the undulator system L . If we consider an electron beam slice with coordinates of (y_0, y_0', z_0) at the undulator entrance, it will experience a continuous vertical kick because of non-zero y_0 , and the vertical motion can be stated as:

$$y'' = -\frac{ek_f}{cm}y \quad (4)$$

Where e , m are the charge and mass of an electron and c is the speed of light. Considering that the vertical motion of this slice is under well control in the whole undulator, i.e., the vertical kick given by undulator lattice is supposed to be constant, and then the vertical motion can be expressed as:

$$y(L) = -\frac{ek_f}{2cm}y_0L^2 + y_0'L + y_0. \quad (5)$$

Now in Eq. (5), the first term represents the beam vertical tilt variation induced by the undulator lattice, while the second and the third terms together shows the beam tilt previously produced by the transverse deflector. In general, one can optimize the undulator lattice and transverse deflector parameters to minimize the beam tilt variation in the whole undulator. In our case, the beam tilt amplitude variation can be controlled within 2%.

3. Simulation results

In this work, the dimensionless undulator parameter K_0 is 1.47 and the undulator period is 15 mm, which leads an FEL resonant wavelength of 0.1 nm. When substituting these parameters into Eq. (3), one can derive the full FEL bandwidth

$$\frac{\Delta\lambda}{\lambda_0} [\%] \approx 2.73y^2 [mm^2] \quad (6)$$

The theoretical expression in Eq. (6) indicates that the produced FEL bandwidth is proportional to the square of vertical tilt amplitude. Now it is obvious that a beam with different tilt amplitude travelling through the planar undulator will produce FEL pulse with different bandwidth. Besides, numerical simulations also have been performed with GENESIS (Reiche, 1999) to further investigate the cases and compare with the theoretical studies, in which a flat-top beam current is assumed.

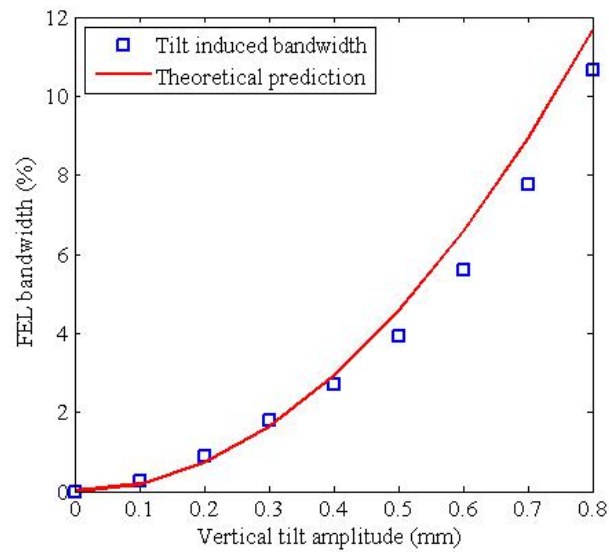


Figure 4

FEL bandwidth after 10 m undulator versus the beam vertical tilt amplitude.

Time-dependent FEL simulations using different beam tilt amplitude are carried out to emulate the produced bandwidth. Figure 4 shows the full bandwidth after 10 m undulator where FEL just turns into the exponential gain region, far from saturation. The blue squares show the bandwidth induced by the beam vertical tilt, which is calculated from the gross bandwidth from simulation and the intrinsic 0.5% bandwidth contributed by the spontaneous emission. In accordance with Eq. (6), it is not difficult to find that the net bandwidth is proportional to the square of beam tilt amplitude. Under this circumstance, the output bandwidth may beyond 10% with a 10 m planar undulator when an electron beam with 0.8 mm vertical tilt amplitude is used.

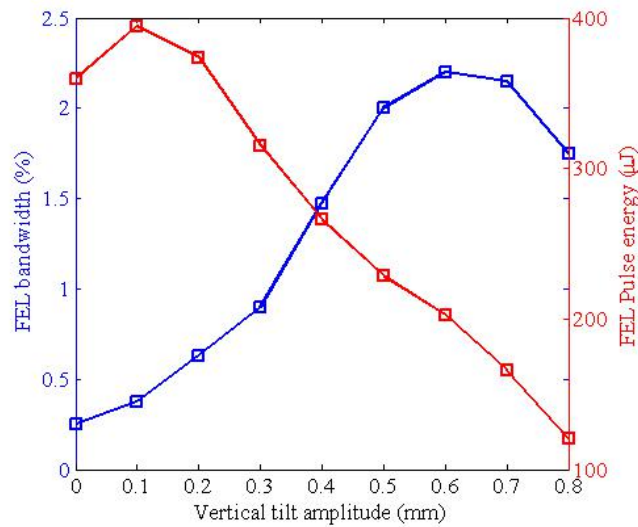


Figure 5

FEL bandwidth and pulse energy of 0.1 nm SASE at saturation.

A typical hard X-ray FEL undulator length is 100 m. After such an undulator, as illustrated in Fig.5, FEL pulse energy and accompanied bandwidth as a function of the vertical beam tilt amplitude has been simulated. Generally, the behaviour of FEL pulse energy is reversed to the evolution of FEL bandwidth. For the pulse energy, it achieves a maximum of 395 μJ when the beam tilt amplitude is 0.1 mm. In this case, the 0.1 mm beam tilt occasionally serves as an undulator taper for some appropriate part of the electron bunch. Then the pulse energy reduces approximately linearly with the increasing beam tilt amplitude, which can be easily understood. On the other hand, regarding to the bandwidth, it grows steadily from the initial 0.25%, and in particular reaches to maximum bandwidth of 2.2% at ± 0.6 mm beam tilt. It is believed that, the electron beam is too much stretched to support a fruitful colour FEL lasing after ± 0.6 mm vertical tilt and the bandwidth draws back. From the practice of view, it is our goal to achieve broad bandwidth even sacrifices some pulse energy. If a beam tilt of ± 0.5 mm can be afforded routinely, an FEL with pulse energy exceeding 200 μJ and bandwidth up to nearly 2.0% can be delivered to users at 0.1 nm wavelength.

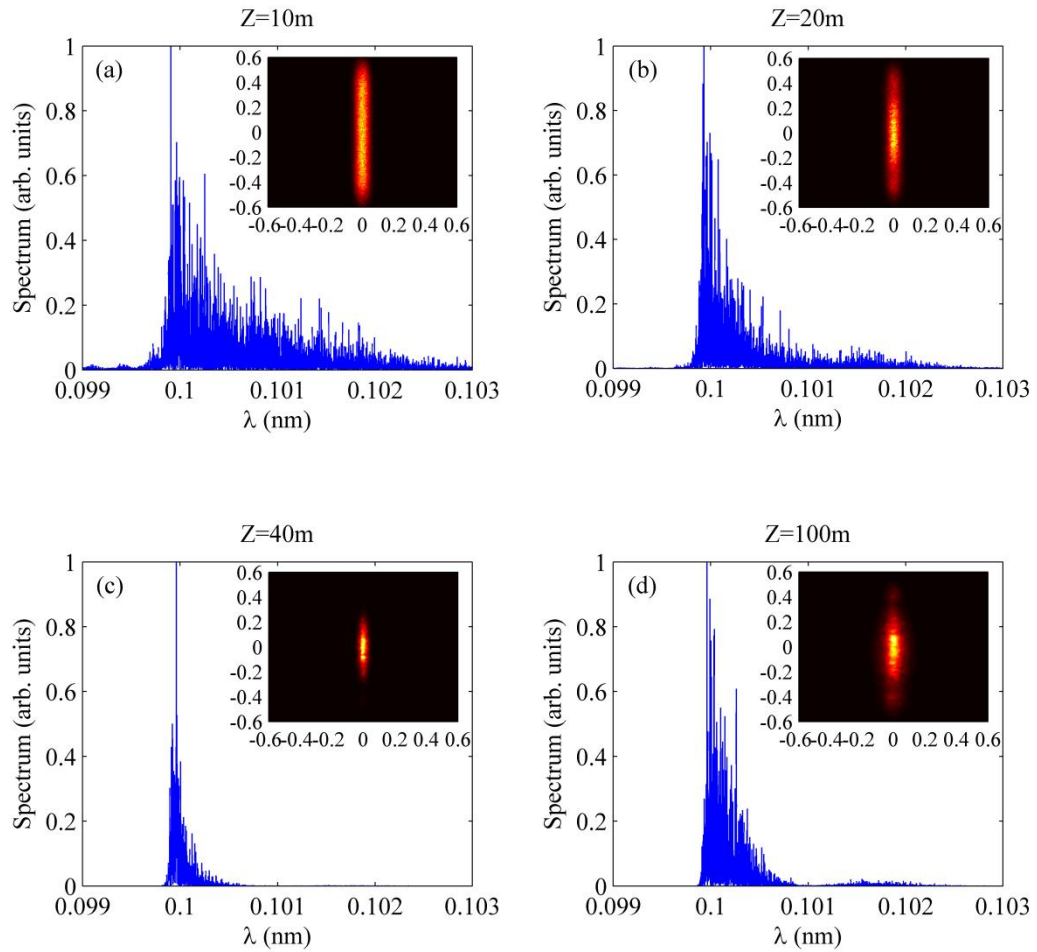


Figure 6

Simulated spectrum and transverse profile of an XFEL pulse along the undulator: the four plots from (a) to (d) represent the four different locations of undulator.

With a vertical beam tilt of ± 0.5 mm, now we consider the radiation spectrum and spot evolution in the undulator, as presented in Fig. 6. Obviously, at the undulator position $Z=10m$, the generated spectrum in Fig. 6 (a) shows a bandwidth about 4%, and the radiation profile with a vertical envelope of 0.5 mm is consistent with the beam vertical tilt amplitude. Then as the electron beam continues to travel in the undulator, the radiation bandwidth gradually decreases. For instance, Fig. 6 (b) describes the radiation properties at the undulator position $Z=20$ m, i.e., in the exponential growth region. It can be found that the spectral bandwidth is narrowed and the radiation vertical size becomes shorter. Until the FEL lasing finally saturates which is presented in Fig. 6 (c), indeed, that FEL bandwidth sharply narrows to 1.25%, meanwhile, the vertical size of FEL spot goes to 0.2 mm which is much smaller than

the initial situation. However after the saturation, as displayed in Fig. 6 (d), it is interesting to note that there is an increase of FEL bandwidth and enlarge of FEL vertical profile, accompanied with blurred periphery. At the exit of the undulator where $Z=100$ m, a FEL bandwidth of 2.0% and vertical FEL size approximately of 0.3 mm is obtained from simulation.

4. Further bandwidth enhancement

In previous study, a 0.1 nm FEL with bandwidth of 2.0% was numerically demonstrated at saturation. It is worth stressing that, for the scheme in Fig.1, the bandwidth can be further increased with control of the beam current distribution and the beam central offset.

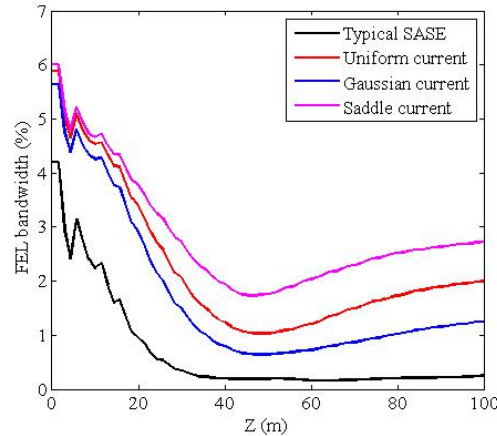


Figure 7

FEL bandwidth evolutions along the undulator regarding to different bunch current distribution.

The blue curve of Fig. 7 displays the bandwidth evolution along the undulator under the vertical beam tilt amplitude equal to 0.5 mm, with the assumption of uniform or flat-top bunch current distribution. In principle, there exists several factors which contribute to the FEL bandwidth reduction along the undulator, e.g., the X-ray diffraction around the two edges which is usually larger than that of the centre are not compensated on time, and the electron exchange in the vertical plane cannot be avoided. More importantly, according to the Eq. (3), the FEL wavelength is determined by the square of beam vertical offset. Then if the electron beam has a vertical tilt amplitude of 0.5 mm, those electrons with the vertical

position between 0.4 and 0.5 mm is responsible for producing 36% of the total bandwidth, while this part of beam only has 20% electrons under a flat-top current distribution assumption. Under such circumstance, it cannot afford a sufficient gain during the exponential growth when compared with those electrons in the centre, and leads a poor brightness of the 36% bandwidth. Therefore, there exists a sharp FEL bandwidth reduction before the initial saturation. After that, with the continuous gain of those unsaturated wavelength, the bandwidth experiences a slightly gradual growth. From the analysis, it is easy to figure out that an effective method to increase FEL bandwidth is using a saddle beam current distribution, and thus those insufficient FEL gain may be enhanced by the high current in the double horn. In modern FEL facilities, due to the bunch compression, a saddle bunch profile is a typical operation mode (Reiche *et al.*, 2005). For comparison, the Gaussian and saddle current distribution are taken into consideration and simulated. According to the plots in Fig. 7, it is definitely demonstrated that the saddle current beam achieve a bandwidth of 2.75%, while the Gaussian beam can only offer a bandwidth of 1.25%. When compared with typical SASE bandwidth of 0.25 % in the hard X-ray region (see the black curve in Fig. 7), it is enhanced by one order of magnitude and could be applied in a wide range of scientific researches.

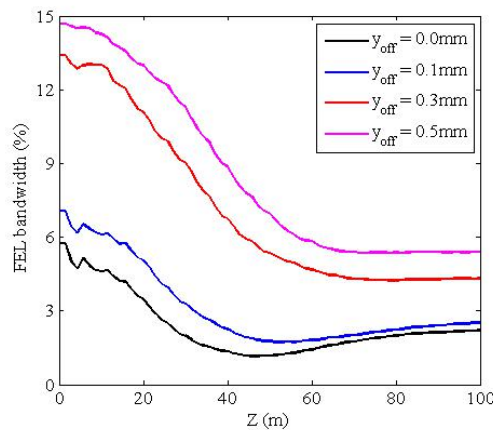
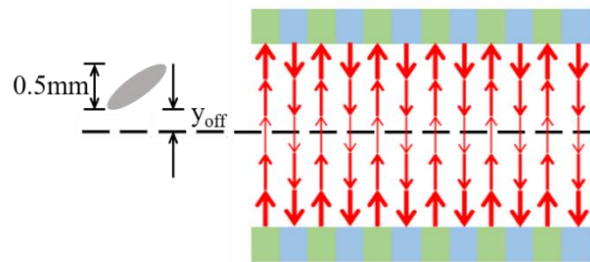


Figure 8

FEL bandwidth evolutions along the undulator regarding to different vertical beam offset.

Now it is clear that the key issue to produce large bandwidth in the proposed scheme is to afford the sufficient and comparable FEL gain for all the wavelengths covered. In the previous discussions, an electron beam on axis was considered, i.e., the electron distributed symmetrically in the vertical plane. In this case, as an example, those electrons around ± 0.4 mm contribute to the same wavelength while they lased at different position and thus reduced the electron density and FEL gain. Therefore, an off-axis electron beam will be studied here, as y_{off} defined in Fig. 8, different vertical offset cases are also considered to avoid the small wavelength variation region around the vertical axis and thus effectively generate the large bandwidth. According to Fig. 8, it is found that an off-axis electron beam is very helpful. After some brief optimization, the FEL bandwidth could achieve 4.2% and 5.3% for the cases $y_{\text{off}} = 0.3$ mm and 0.5 mm, respectively. When compared with typical SASE bandwidth, it is enhanced by more than 20 times, and could be applied in efficient X-ray absorption spectroscopy and magnetic circular dichroism (Deng *et al.*, 2017).

5. Conclusion

Typically, the FEL sources aim to pursue the narrow bandwidth radiation. However, there is a strong demand to generate large bandwidth X-ray FEL pulse for several scientific applications. Therefore, in this paper, under the optimized undulator lattice, a transversely tilted beam is sent through the planar undulator with natural gradient to achieve the broad bandwidth FEL pulse. The electron beam vertical tilt can be obtained by the transverse wakefields of corrugated structure or a deflecting cavity, and then the FEL bandwidth is expected to be simply controlled by variation of the corrugated structure gap or the deflecting voltage. The numerical simulation confirmed the validity of the scheme and theoretical analysis used in this paper. It is demonstrated that, the proposed scheme is able to deliver 0.1 nm FEL pulse with bandwidth from 2.0% to 5.0%, corresponding to different beam current profiles and beam offset. It is found that, during the FEL process, the produced radiation bandwidth sharply drops during the exponential growth, which is mainly caused by the unfair

gains for different colour radiations. Thus in some user experiments, if they does not care the X-ray photon numbers that much, X-ray pulses with intensity much higher than spontaneous emission and bandwidth more than 10% could be afford. More importantly, the novel scheme proposed here relies on the mature accelerator technique and the existing devices in modern short-wavelength FEL facilities. It paves the way for experiments requiring large bandwidth or multi-colour X-ray FEL pulse.

References

- Ackermann, W., Asova, G., Ayvazyan, V. *et al.* (2007). *Nat. Photon.* **576**, 675-82.
- Akre, R., Bentson, L., Emma, P., & Krejcik, P. (2001). *A transverse RF deflecting structure for bunch length and phase space diagnostics*. Report PUB-8864. SLAC National Accelerator Laboratory, SLAC, USA.
- Alesini, D., Pirro, G. D., Ficcadenti, L. *et al.* (2006). *Nucl. Instrum. Methods Phys. Res. A*, **568**, 488–502.
- Amann, J. *et al.* (2012). *Nat. Photon.* **6**, 693–698.
- Andonian, G., Murokh, A., Rosenzweig, J. B. *et al.* (2005). *Phys. Rev. Lett.* **95**, 054801.
- Baradaran, R. *et al.* (2013). *Nat. Photon.* **494**, 443-448.
- Barletta, A. W., Bisognano, J., Corlett, J. N. *et al.* (2010). *Nucl. Instrum. Methods Phys. Res. A*, **618**, 69-96.
- Bane, K., Stupakov, G., & Zagorodnov, I. (2016). *Phys. Rev. ST Accel. Beams*, **19**, 084401.
- Bernhard, A., Braun, N., Rodríguez, V. A. *et al.* (2016). *Phys. Rev. ST Accel. Beams*, **19**, 090704.
- Berrisford, J. M., Minhas, G. S. *et al.* (2013). *Nat.* **494**, 443-448.
- Bonifacio, R., Pellegrini, C., Narducci, L. M. (1984). *Opt. Commun.* **50**, 373-378.
- Borland, M. (2000). *A flexible SDDS-compliant code for accelerator simulation*. Report LS-287. Argonne National Lab, IL, US.
- Catherine, D. *et al.* (2015). *IUCrJ.* **2**, 361–370.
- Cornacchia, M., & Emma, P. (2002). *Phys. Rev. ST Accel. Beams*, **5**, 084001.
- Deng, H., & Feng, C. (2013). *Phys. Rev. Lett.* **111**, 084801.
- Deng, H., Zhang, M., Feng, C. *et al.* (2014). *Phys. Rev. Lett.* **113**, 254802.

Ding, Y. *et al.* (2014). *Results from the LCLS x-band transverse deflector with femtosecond temporal resolution*. Report PUB-16105. SLAC National Accelerator Laboratory, SLAC, USA.

Emma, P., Akre, R., Arthur, J. *et al.* (2010). *Nat. Photon.* **4**, 641-647.

Emma, P., Venturini, M., Bane, K. L., Stupakov, G. *et al.* (2014). *Phys. Rev. Lett.* **112**, 034801.

Emma, P. (2000). *Chirping the LCLS electron beam*. Technical Report LCLS-TN-00-6. SLAC National Accelerator Laboratory, SLAC, USA.

Fu, F., Wang, R., Zhu, P. *et al.* (2015). *Phys. Rev. Lett.* **114**, 114801.

Hernandez, A. S., Prat, E., Bettoni, S., Beutner, B., & Reiche, S. (2016). *Phys. Rev. ST Accel. Beams*, **19**, 090702.

Huang, Z., & Kim, K. J. (2007). *Phys. Rev. ST Accel. Beams*, **10**, 034801.

Ishikawa, T., Aoyagi, H., Asaka, T. *et al.* (2012). *Nat. Photon.* **6**, 540-544.

Jia, Q. K., Zhang, S., Lu, S. *et al.* (2004). *Proceedings of the 25th International Free-Electron Laser Conference*, pp. 494-497.

Kondratenko, A. M. & Saldin, E. L. (1980). *Part. Accel.* **10**, 207-216.

Korepanov, S., Khodyachykh, S., Krasilnikov, M., Oppelt, A., & Stephan, F. (2006). *Proceedings of the Russian Particle Accelerator Conference*, pp. 247-249.

Lee, H. J., Han, J-H. *et al.* (2014). *Proceedings of the 35th International Free-Electron Laser Conference*, pp. 707-709.

Lutman, A. A., Maxwell, T. J., MacArthur, J. P. *et al.* (2016). *Nat. Photon.* **10**, 745-750.

Madey, J. M. J. (1971). *J. Appl. Phys.* **42**, 1906-1913.

Novokhatski, A. (2015). *Phys. Rev. ST Accel. Beams*, **18**, 104402.

Öström, H., Öberg, H., Xin, H. *et al.* (2015). *Sci.* **347**, 978-982.

Park, S., Kim, E. S. *et al.* (2015). *Proceedings of the 36th International Free-Electron Laser Conference*, pp. 188-190.

Patterson, J. C., Klimenko, E. S., Thorner, J. (2010). *Sci. Signal.* **3**, 625-638.

Penco, G., Danailov, M., Demidovich, A. *et al.* (2014). *Phys. Rev. Lett.* **112**, 044801.

Prat, E., Calvi, M., Reiche, S. (2016). *J. Synchrotron Rad.* **23**, 874-879.

Reiche, S. (1999). *Nucl. Instrum. Methods Phys. Res. A*, **429**, 243-248.

- Reiche, S., Bane, K., Emma, P., Huang, Z. *et al.* (2005). Optimization of the LCLS x-ray FEL output performance in the presence of strong undulator wakefields. Report PUB-11773. SLAC National Accelerator Laboratory, SLAC, USA.
- Saldin, E. L., Schneidmiller, E. A., Shvyd'ko, Y. V. & Yurkov, M. V.(2001). *Nucl. Instrum. Methods Phys. Res. A*, **475**, 357–362.
- Serkez, S., Kocharyan, V., Saldin, E., Zagorodnov, I., Geloni, G. & Yefanov, O. (2013). *Extension of SASE bandwidth up to 2% as away to increase the efficiency of protein structure determination by X-ray nanocrystallography at the European XFEL*. Report 13–109. Deutsches Elektronen-Synchrotron, Hamburg, Germany.
- Son, S.-K., Chapman, H. N. & Santra, R. (2011). *Phys. Rev. Lett.* **107**,218102.
- Stupakov, G. (2009). *Phys. Rev. Lett.***102**, 074801.
- Tan, J., Gu, Q., Fang, W., Tong, D., Zhao, Z., (2014). *Nuclear Science and Techniques*, **25**, 060101.
- Turner, J. L. *et al.* (2015). *Proceedings of the 36th International Free-Electron Laser Conference*, pp. 337–341.
- Wiedemann, H. (2008). *Particle Accelerator Physics*. pp. 238–280 New York: Springer.
- Xiang, D., & Ding, Y. (2010). *Phys. Rev. ST Accel. Beams*, **13**, 094001.
- Xie, M. (1995). *Proceedings of the IEEE*, pp.183-185.
- Yu, L. (1991). *Phys. Rev. A*. **44**, 5178-5193.
- Zagorodnov, I., Bane, K. L. F., & Stupakov, G. (2015). *Phys. Rev. ST Accel. Beams*, **18**, 104401.
- Zhang, Z., Bane, K., Ding, Y., Huang, Z., Iverson, R., & Maxwell, T. *et al.* (2015). *Phys. Rev. ST Accel. Beams*, **18**, 010702.
- Zhao, Z., Wang, D., Chen, J.*et al.* (2012). *Nat. Photon.* **6**, 360-363.
- Deng, B., Zhang, Q. *et al.* (2017). *Private communication*.